Journal of Computer-Aided Molecular Design, **15:** 1137–1152, 2001.
KLUWER/ESCOM

Reproducing the conformations of protein-bound ligands: A critical evaluation of several popular conformational searching tools

Jonas Boström
Department of Medicinal Chemistry, AstraZeneca R&D Mölndal, Sweden

Received 18 June 2001; accepted 7 February 2002

Key words: bioactive conformation, Catalyst, comparison, conformational analysis, Confort, Flo99, high-resolution X-ray crystallography, MacroModel, Omega

Summary

Several programs (Catalyst, Confort, Flo99, MacroModel, and Omega) that are commonly used to generate conformational ensembles have been tested for their ability to reproduce bioactive conformations. The ligands from thirty-two different ligand–protein complexes determined by high-resolution ($\leq$2.0 Å) X-ray crystallography have been analyzed. The Low-Mode Conformational Search method (with AMBER* and the GB/SA hydration model), as implemented in MacroModel, was found to perform better than the other algorithms. The rule-based method Omega, which is orders of magnitude faster than the other methods, also gave reasonable results but were found to be dependent on the input structure. The methods supporting diverse sampling (Catalyst, Confort) performed least well. For the seven ligands in the set having eight or more rotatable bonds, none of the bioactive conformations were ever found, save for one exception (Flo99). These ligands do not bind in a local minimum conformation according to AMBER*\GB/SA. Taking these last two observations together, it is clear that geometrically similar structures should be collected in order to increase the probability of finding the bioactive conformation among the generated ensembles. Factors influencing bioactive conformational retrieval have been identified and are discussed.

Introduction

For a ligand to bind to a receptor, and thereby initiate a biological effect, it generally has to adopt a conformation which is in some way complementary to its target protein. This protein-bound conformation is termed the *bioactive* conformation. It is often a non-trivial task to determine the bioactive conformation, since most drug-like molecules have numerous low-energy conformations.

The determination of bioactive conformations is an important challenge for computer-aided ligand design. For example, a deduced bioactive conformation may be used to gain knowledge about the ligand–protein complex, and thus be used as a template when designing novel compounds with desired properties. To obtain reliable results when performing procedures such as 3D-database searching [1], rigid-fit pharmacophore modeling [2], and docking studies [3], the bioactive conformation has to be included in the conformational ensemble employed. Representative conformational ensembles, i.e. those which contain the bioactive conformation, are also of the utmost importance when performing 3D-QSAR studies using multiple alignments [4]. Moreover, accurate conformational ensembles may also be of assistance in cases where a single ligand conformation cannot be unambiguously assigned to an X-ray electron density.

The optimal way of determining a ligand's protein-bound conformation is of course by experiment, e.g., high-resolution X-ray crystallography. However, this is time-consuming and not always successful. The next best thing is to use a computational approach starting with a conformational ensemble including the bioactive conformation. Today, several methods are available for generating conformational ensembles. However, the problem is not *how to generate* a confor-

*Corresponding author: E-mail: jonas.bostrom@astrazeneca.com; Tel: +46 31 706 52 51; Fax: +46 31 776 37 10

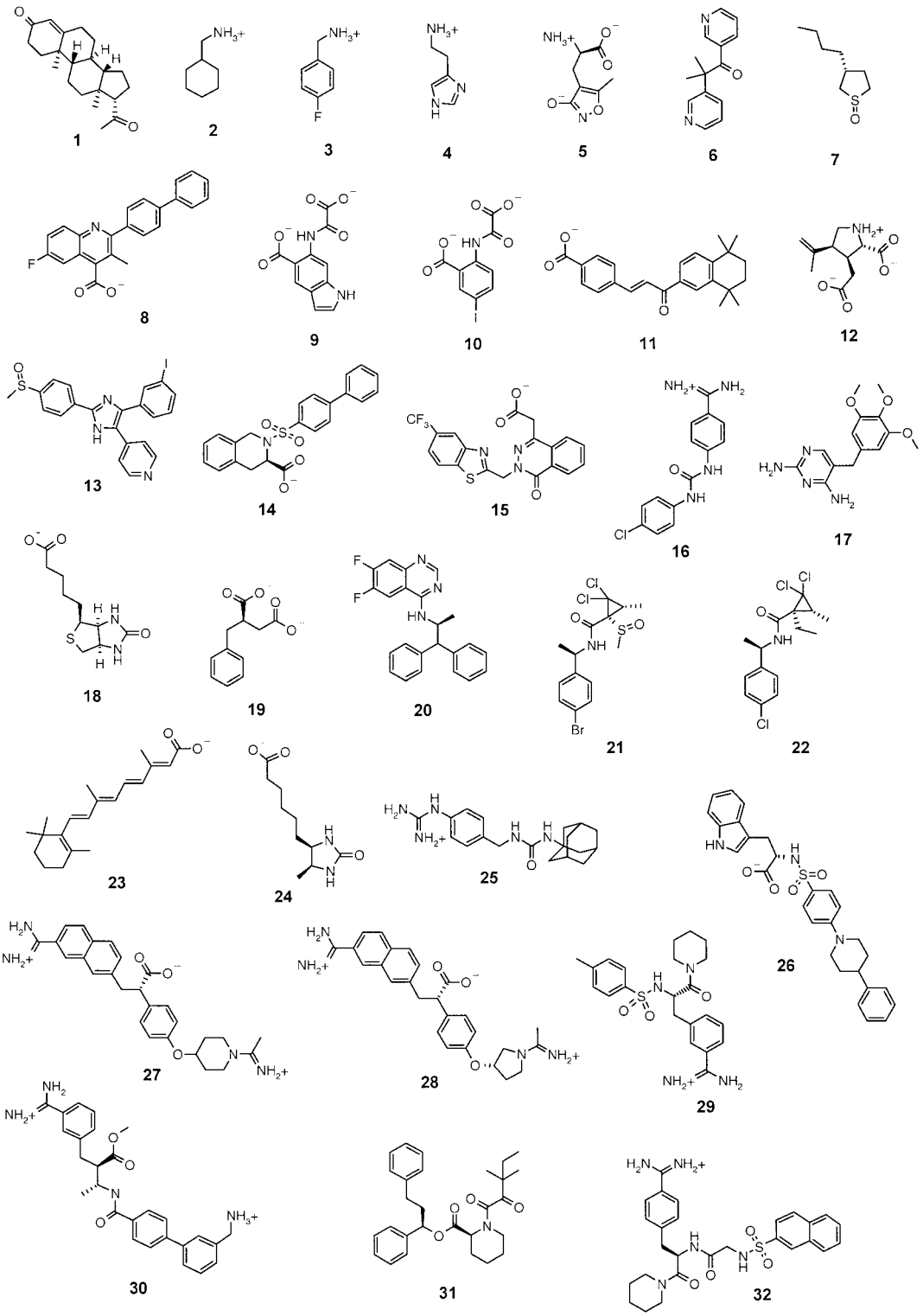

Figure 1. Structures of the ligands studied in this work.

mational ensemble, but *how to choose* which method is likely to give the best results.

Conformational search procedures are typically validated against standard benchmark data sets. In one typical approach, several experimental conformational distributions are used to judge both the number of conformations generated by the method, as well as their relative energies. An alternative approach is to compare generated conformations against small molecule X-ray structures taken from the Cambridge Crystallographic Database [5]. Sadowski et al. found that the Corina program [6] reproduced the correct conformation for nearly half of their data set of 639 X-ray structures [7]. Treasurywala et al. analyzed stochastic searching techniques available in MacroModel [8] and SYBYL [9], though the results were not definitive [10]. For an extensive review on conformational analysis the reader is referred to reference 11.

Now that the number of high-resolution X-ray protein-ligand complexes included in the Brookhaven Protein Data Bank [12] is increasing rapidly, a third approach presents itself. Namely, it has become possible to determine whether experimentally determined bioactive conformations are present in various generated conformational ensembles. Nevertheless, a comprehensive comparison of the ability of various conformational search tools to reproduce X-ray receptor-bound conformations has not yet been published. It must be stressed that it is vital to use high-quality complexes when performing a detailed study like this one.

The aim of the present study is to evaluate several methods that are commonly used to generate conformational models for their reliability in reproducing bioactive conformations. In other words, we examine whether or not the ligand X-ray conformation is present in the various conformational ensembles produced by computation.

Methods

Selection of ligand-protein complexes

The ligands used in this study were taken from the Brookhaven Protein Data Bank. ReLiBase was used as a valuable tool for selecting the molecules [13]. Several criteria were used to choose an accurate and representative set of molecules: (i) the X-ray structure resolution should be high, less than or equal to 2.0 Å; (ii) the temperature ('B') factors of the ligands must be low, preferably below 30; (iii) the ligands must not include rotatable bonds that can not be detected by protein crystallography, e.g., hydroxyl torsions, (iv); the ligands should not include unusual or poorly parameterized moieties (v) they should be reasonably small, flexible and 'drug-like'. Thirty-two ligands were selected. The ligands in the set have from one to eleven freely rotatable bonds, with a roughly even distribution over this range. The protonation states of the molecules, which is the prevalent species at physiological pH, were used in the calculations. Data for the ligands are given in Table 1 and the molecular structures are shown in Figure 1.

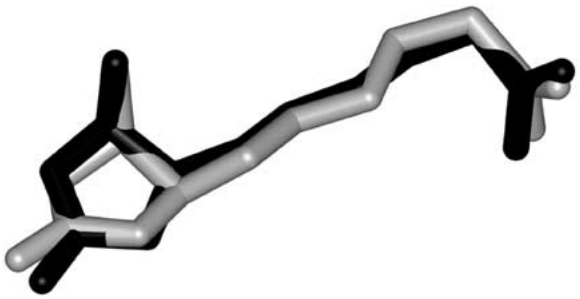

Figure 2. (a) A least-squares superposition of the unmodified X-ray structure of the protein-bound ligand **24** (grey) and the corresponding best hit (black) in the conformational ensemble generated by Omega. The RMSD value is 0.46 Å – a hit. Hydrogens are removed for clarity.

When is an X-ray structure considered to be reproduced?

Because the unmodified X-ray structure of the protein-bound ligands is compared to conformations obtained from conformational analysis, it is crucial that the ligand-protein complexes have been determined to a very high resolution. The resolution of the complexes must be sufficient to unambiguously provide the bioactive conformation. However, crystal structures of proteins are rarely determined to atomic resolution. As a rule of thumb, the positional error amounts to about one-sixth of the resolution. In this study, the resolution of the chosen complexes lies between 1.4 and 2.0 Å, with an average resolution of 1.8 Å. This means, by a crude measure, that the atomic positions are subject to an error of approximately 0.3 Å. However, in some cases high resolution alone may not be enough. Several cases show that even though the resolution of the ligand-protein complex is high, the ligand atomic positions may be severely ill defined (see below).

Table 1. The ligands, the PDB code, crystallographic parameters and the protein in the ligand–protein complex.

No.	PDB code	Ligand	Resolution (Å)	R-factor	B-Factor[a]	Protein
1	1a28	Progesterone	1.80	0.191	20–32	Progesterone receptor
2	1tng	Aminomethylcyclohexane	1.80	0.172	10–20	Trypsin
3	1tnh	*p*-Fluoro-benzylamine	1.80	0.168	10–25	Trypsin
4	1qft	Histamine	1.25	0.184	9–11	Histamine-binding protein
5	1ftm	AMPA	1.70	0.210	7–15	Glutamate receptor-2
6	1phg	Metyrapone	1.60	0.190	12–19	Cytochrome P450-cam
7	3bto	3-Butyl-thiolane-1-oxide	1.66	0.207	12–21	Liver alcohol dehydrogenase
8	1d3g	2-Biphenyl-4-yl-6-fluoro-3-methyl-quinoline-4 carboxylic acid	1.60	0.168	17–24	Human dihydroorotate dehydrogenase
9	1c83	6-(Oxalyl-amino)-1*H*-indole-5-carboxylic acid	1.80	0.197	8–12	Tyrosine phosphatase 1B
10	1ecv	5-Iodo-2-(oxalyl-amino)-benzoic acid	1.95	0.194	7–26	Tyrosine phosphatase 1B
11	1fcz	BMS181156	1.38	0.132	13–24	Retinoic acid nuclear receptor
12	1gr2	Kainate	1.90	0.216	9–14	Glutamate receptor-2
13	1ian	4-[5-(3-Iodo-phenyl)-2-(4-methanesulfinyl-phenyl)-1*H*-imidazole-4-yl]-pyridine	2.00	0.234	13–34	P38 Map kinase
14	1bzs	2-(Biphenyl-4-sulfonyl)-1,2,3,4-tetrahydro-isoquinoline-3-carboxylic acid	1.70	0.192	5–27	Neutrophil collagenase
15	1frb	3,4-Dihydro-4-oxo-3-((5-trifluoromethyl-2-benzothiazolyl)methyl)-1-phthalazine acetic acid	1.70	0.158	2–13	Fr-1 Protein
16	1bju	1-(4-Amidinophenyl)-3-(4-chlorophenyl)urea	1.80	0.171	9–31	Trypsin
17	1dyr	Trimethoprim	1.86	0.181	10–20	Dihydrofolate reductase
18	2izg	Biotin	1.36	0.206	15–23	Streptavidin
19	1cbx	L-Benzylsuccinate	2.00	0.166	5–21	Carboxypeptidase A
20	5std	(6,7-Difluoro-quinazolin-4-yl)-(1-methyl-2,2-diphenyl-ethyl)-amine	1.95	0.212	11–23	Scytalone dehydratase
21	6std	2,2-Dichloro-1-methanesulfinyl-3-methyl-cyclopropanecarboxylic acid [1-(4-bromo-phenyl)-ethyl]-amide	1.80	0.195	18–29	Scytalone dehydratase
22	7std	Carpropamide	1.80	0.197	2–24	Scytalone dehydratase
23	1cbs	Retinoic acid	1.80	n.a.[b]	9–16	Retinoic acid binding protein
24	1dam	6-(5-Methyl-2-oxo-imidazolidin-4-yl)-hexanoic acid	1.80	0.180	15–25	Dethiobiotin synthetase
25	1ejn	*N*-(1-Adamantyl)-*N′*-(4-guanidinobenzyl)urea	1.80	0.200	17–32	Urokinase
26	1caq	3-(1*H*-Indol-3-yl)-2-[4-(4-phenyl-piperidin-1-yl)-benzenesulfonylamino]-propionic acid	1.80	0.193	12–22	Stromelysin-1
27	1mtv	(+)-2-[4-[(-1-Acetimidoyl-4-piperidinyl)oxy]-3-(7-amidino-2-naphthyl)propionic acid	1.90	0.169	10–32	Trypsin

[a]Interval for the ligand temperature factors. [b]R value not available.

Table 1. Continued.

No.	PDB code	Ligand	Resolution (Å)	R-factor	B-Factor[a]	Protein
28	1mtw	(+)-2-[4-[((S)-1-Acetimidoyl-3S-pyrrolidinyl)oxy]-3-(7-amidino-2-naphthyl)propionic acid	1.90	0.169	6–29	Trypsin
29	1ppc	NAPAP	1.80	0.181	14–31	Trypsin
30	1f0u	RPR128515	1.90	0.172	11–29	Trypsin
31	1fkg	(1R)-1,3-Diphenyl-1-propyl (2S)-1-(3,3-dimethyl-1,2-dioxopentyl)-2-piperidinecarboxylate	2.00	0.184	2–17	Fk506 binding protein
32	1pph	3-TAPAP	1.90	0.167	8–23	Trypsin

[a]Interval for the ligand temperature factors. [b]R value not available.

Structures are generally considered to be the same unless the least-squares superimposition of the compared atoms finds one or more pairs of equivalent atoms separated by more than 0.25–0.30 Å [7, 8]. In this study a slightly more tolerant cut-off was used. That is, a hit is defined as a conformation of 0.5 Å or less from the unmodified X-ray structure. Figure 2 shows a least-squares superposition of the unmodified X-ray structure **24** (grey) and the corresponding best conformation (black) in the conformational ensemble generated by Omega [14], as a representative example. The RMSD value is 0.46 Å.

Computational methods

The conformational search methods

The programs evaluated in this study are Catalyst [15], Confort [16], Flo99 [17], MacroModel [8], and Omega [14]. The conformational ensembles were sampled with default settings in order to reflect normal usage. A short description of the methods used and the parameters controlling ensemble size for each method are given in the next few sections.

Catalyst v 4.6.
Catalyst supports two methods of conformational generation termed BEST and FAST. Fundamental to Catalyst is the so-called poling algorithm [18]. It is designed to sample as diverse a set of conformations as possible. Thus, both BEST and FAST stress coverage of conformational space. BEST is reported to be more thorough, in particular when handling flexible ring systems. FAST is more approximate, and therefore requires substantially less CPU time. Catalyst uses the CatalystCHARMM force field, which does not include any electrostatic terms. BEST employs conjugate-gradient minimization in both torsion and Cartesian space, in conjunction with poling. The default setting is to collect a maximum of 250 conformations within an energy cut-off of 20 kcal/mol.

Confort v3.9.
Confort relies on an algorithm that performs a truly exhaustive search of the conformational space. The user has the option to sample either a defined number of low-energy conformations or a diverse set of conformers. In the present study only the latter method is evaluated. There are two ways to discard high-energy conformers while searching for diverse conformations. The first method uses an 'intermediate' energy window. This might result in a reduction of conformational diversity. The second method uses a 'final' energy window, with the possibility of reducing the number of output conformations below what was requested. The diverse sampling is based on a so-called refinement procedure. Functions of interatomic distances are optimized instead of performing energy minimizations. Accordingly, no duplicate conformations are produced. Confort uses the Tripos force field and its own minimizer. Atomic charges are not used in the calculations. A maximum of 50 conformations or 20 percent of the total number of conformations are sampled when using default settings. Conformations with an energy of more than 5 kcal/mol above the global minimum conformation are discarded.

Flo99.
Conformational searches are carried out based on the wide-angle Metropolis algorithm [19]. To avoid getting trapped in a subset of conformation space, the

Metropolis step is embedded in a loop which starts with a random perturbation of a number of torsion bonds. The maximum number of minimizations is set to the number of rotatable bonds multiplied by 100, and is not allowed to exceed 1500. Any new conformation with an energy of less than 12 kcal/mol (50 kJ/mol) above the current global minimum is stored. A limit of 300 conformations are stored. The molecular mechanics routine (QXP) uses a modified version of the AMBER force field. QXP works with united carbon atoms (no hydrogens necessary). In addition, all electrostatic contributions are turned off during conformational analysis. A modified version of the Polak-Ribiere conjugate gradient minimization is used.

MacroModel v7.0.
Several algorithms for conformational analysis are implemented in MacroModel. The Low-Mode Conformational Search (LMCS) method has proven to be highly efficient and accurate [20], and was therefore chosen. LMCS works by exploring low-frequency eigenvectors of the system, which are expected to follow degrees of freedom with small force constants, such as torsion angles. LMCS is the only method in the present study which may be used with several different force fields and with a hydration model. Redundant conformations are removed by heavy atom superimposition (0.25 Å RMSD). The energy minimizations were carried out using the truncated Newton conjugate gradient algorithm. Any structure with an energy of more than 12 kcal/mol (50 kJ/mol) above the current global minimum are discarded. The maximum number of minimizations is 1000. For each ligand, the conformational analysis was performed in aqueous solution, using the generalized Born/solvent accessible surface area (GB/SA) model [21], as well as *in vacuo*. To check for force field dependence, both MMFF94S and AMBER* were tested.

Omega v 0.9.9.
Omega supports a so-called torsion-driving beam search for generating ensembles of conformers. It is a rule-based method that generates conformations extremely rapidly. By contrast with stochastic methods, the results are completely reproducible. Omega deconstructs the molecule into fragments with rotatable bonds, and uses certain build-up principles to generate a conformational ensemble. Omega does not minimize bond lengths or bond angles. All heavy atoms are superimposed to test for duplicate structures, and an RMS deviation of 0.8 Å is default. Omega includes a simple force field called the Clean force field. Any structure with an energy of more than 10 kcal/mol above the current global minimum is discarded. The default limit is to collect 75 conformations.

Conformational analysis

Two runs for each method were conducted in order to monitor whether the input conformation influences the results. That is, some methods (e.g., stochastic methods) might get trapped in local minima which would cause the results to differ from search to search. Methods such as torsion-driving beam searching (Omega) which do not optimize bond lengths and angles might also be dependent on the input conformation. Two scenarios were assumed, on the basis of typical practice: In the first case, an input conformation was generated from the X-ray structure, finding the closest local minimum using the AMBER* force field in combination with the GB/SA hydration model. This typifies using the X-ray structure as the starting point. In the second case, the protocol was repeated, starting with structures generated with the 2D-to-3D-generator program Corina [6].

The superimposition procedure

All conformations in a given ensemble were superimposed on the corresponding unmodified X-ray structure by a least-squares superimposition procedure. Only non-hydrogen atoms were matched. To remove artificial differences caused by symmetry, the Match3d program was used [22]. For example, the two amidine nitrogens (N_A and $N_{A'}$) in Figure 3a are equivalent. In this case re-numbering is a prerequisite to avoid large RMS deviations for identical conformations. Accordingly, Match3d re-numbers the structures that are fitted to each other. Likewise, the lowest energy conformation of compound **2** may be represented by two forms: −gauche and +gauche (Figure 3b). In this case matching against the mirror image will result in a large RMS deviation for energetically identical conformations. Therefore Match3d matches the X-ray structure with both the image and the mirror image of the generated structure, to obtain the lowest possible RMS deviation. In addition, the superposition procedure has been automated and an interactive web interface was designed, using dynamic HTML documents, to facilitate the interpretation of the results. Virtually all superimpositions have been visually inspected.

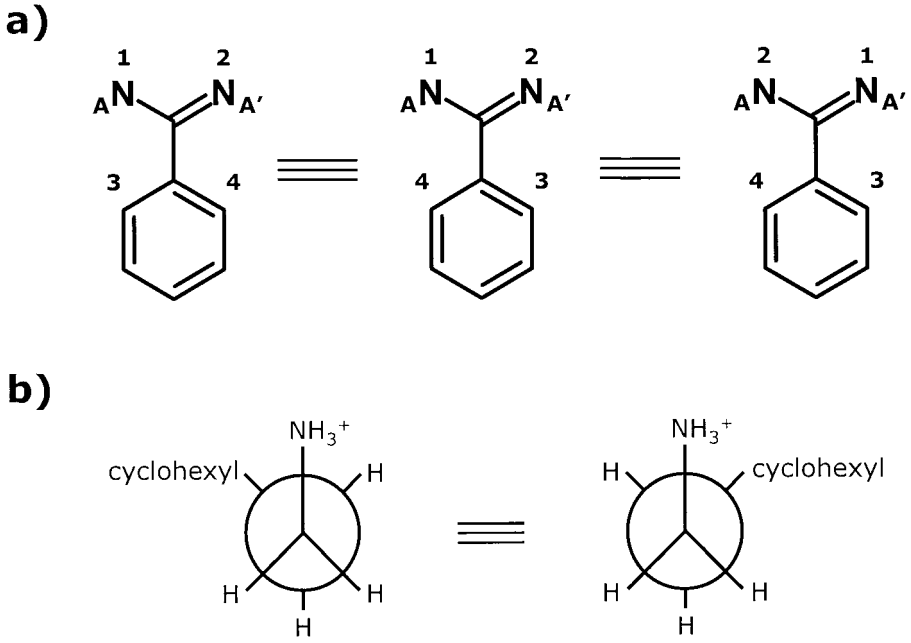

Figure 3. Artificial differences caused by symmetries were removed by using the Match3d program [22]. For example, Match3d re-numbers the structures that are fitted to each other to avoid large RMS deviations. (a) Despite different atom numbering the three structures (and N_A and $N_{A'}$) are identical according to Match3d. (b) Likewise, the lowest energy conformation of compound **2** may be represented by two forms: −gauche and +gauche. Matching against the mirror image will result in a large RMS deviation for energetically identical conformations. Therefore Match3d matches the X-ray structure with both the image and the mirror image of the generated structure, to obtain the lowest possible RMS deviation.

Quantum chemical calculations

Ab initio calculations (HF/6-31G*, Spartan 5.1 [23]) were performed on two conformational energy comparisons: between the X-ray structure, optimized with dihedral angle constraints, and the fully relaxed toluene moiety of 3-phenylpropylamine; and likewise the constrained and fully relaxed phenylmethanesulfinyl moiety of SB-202190 (Figure 2). These calculations were performed to demonstrate the importance of using high-quality X-ray complexes when performing a study like this one. When analyzing the bound conformation of 3-phenylpropylamine and SB-202190 it is clear that the structures contain errors. Accordingly, they are *not* included in the data set. Further interpretations are found under Results and Discussion.

Results and discussion

The importance of X-ray temperature factors as a guide to ligand selection

As mentioned above, crystal structures of proteins are seldom determined to atomic resolution. However, one frequently encounters ligand–protein complexes where the resolution of the complex is high while the quality of the ligand is poor. For example, the resolution of the ligand–protein complex with PDB entry 1pme [24] may be considered high (2.0 Å). However, on visualizing the bound ligand (SB-202190), it becomes clear that part of the structure is wide of the mark, see Figure 4. The methanesulfinyl moiety is planar, rather than the expected pyramidal geometry. The conformational energy difference between the pyramidal and planar forms was calculated to be as high as 41.9 kcal/mol (HF/6-31G*), in favor of the pyramidal form. This high conformational energy is clearly incompatible with the high affinity (31 nM) of SB-202190 binding to P38 Map kinase [25]. The temperature factors for this part of the ligand are slightly higher (>33) than the cut-off used

in this study. Likewise, the resolution of ligand-protein complex 1tnk [26] may be considered very high (1.8 Å). However when analyzing the bound ligand, 3-phenylpropylamine, it is clear that the structure is wrong. The aromatic sp^2 benzene carbon bound to the propylamine moiety is reported to be pyramidal, instead of planar (Figure 4b). The conformational energy for this out-of-plane distortion was determined, to investigate whether this conformation might actually be present in the X-ray structure. The calculations show a large energy difference between the planar and the pyramidal forms, 6.5 kcal/mol (HF/6-31G*), in favor of the planar form. Consequently, the pyramidal form of the bound ligand is unlikely, on account of its unreasonable high energy [25]. The temperature factors for this ligand are higher (>40) than the cut-off allowed here.

Stearic acid, a long-chain fatty acid present in PDB entry 1lif [27], provides an example of where all ligand atoms have fairly high temperature factors (>35). This suggests that the bioactive conformation is an equilibrium of several conformations, rather than a single conformation. That is, although the resolution is very high (1.6 Å), the overall quality of the complex is likely to be insufficient to unambiguously provide a unique bioactive ligand conformation. Several different conformations of stearic acid probably fit the X-ray electron density map.

Statistics

As mentioned above, the conformational ensembles were sampled with default settings to reflect everyday usage. Tables 2 and 3 report the best fits of ligands **1**–**32**, as defined by lowest RMS deviation, according to all methods. A hit is indicated with grey background color. Tables 2 and 3 also show the overall timings and the average number of conformations for each method. In Tables 4 and 5, the calculated values are grouped into 0.25 Å intervals. These tables give the number of structures in each of these intervals. Tables 2 and 4 shows the results obtained when the input structures were X-ray derived. Tables 3 and 5 shows the results obtained when the input structures were derived by the 2D-to-3D conversion program Corina.

MacroModel

Fewer than half of the bioactive conformations were found in the gas phase MMFF94S ensembles (Tables 2 and 3). Five compounds **4**, **5**, **12**, **19** and **22** which were not in these ensembles were found by using the same force field in conjunction with the GB/SA hydration model. Four of these compounds (**4**, **5**, **12** and **22**) contain potential intramolecular hydrogen bonds (NH–N, NH–O or NH–Cl). In these cases, a folded conformation is much more energetically favorable than an extended conformation. Transferring the molecules into solvent tempers these intramolecular interactions. In aqueous solution there is competition between solute–solvent interactions and intramolecular hydrogen bonds. This competition reduces the energy difference between the folded and the extended forms.

To illustrate, the global minimum of compound **4** (Figure 5a) is calculated to be folded both in gas phase and in solution according to the MMFF94S force field. The energy difference between the lowest energy conformation and the bioactive conformation (Figure 5b) in gas phase is 13.4 kcal/mol. Since the energy cut-off is 12 kcal/mol, the bioactive conformation would not be found in the gas phase ensemble. Due to the competition between solute–solvent interactions and intramolecular hydrogen bonds, the corresponding energy difference is only 1.5 kcal/mol when using the GB/SA hydration model, which is well within the defined energy cut-off. Thus, it is clear that using the hydration model increases the hit-rate (Tables 2 and 3).

Among all the compared methods, MMFF94S\GB/SA was found to retrieve all bioactive conformations within the lowest RMSD interval (Tables 4 and 5). The RMSD value for the worst fit was 1.23 Å (compound **28**, Tables 2 and 3).

When using AMBER* in combination with the hydration model, twenty-two of the thirty-two ligands were found (Tables 2 and 3). This is the highest hit-rate among all the compared methods. The compounds which failed to turn up in the AMBER*\GB/SA ensembles were **13**–**15**, along with the seven ligands with eight or more rotatable bonds (**26**–**32**). These were investigated further. All X-ray structures were relaxed two times. First, flat bottom Cartesian constraints were used to ensure that the relaxed conformation did not deviate by more than 0.5 Å from the unmodified X-ray conformation. The energies of the relaxed conformations were recorded, relative to the global minima. In each case, the relative energies were well within the energy threshold. Consequently, it is *not* the energy cut-off which is causing the absence of the bioactive conformations from the ensembles. Secondly, the X-ray structures were relaxed to their closest local minima. The RMSDs with respect to the unmodi-

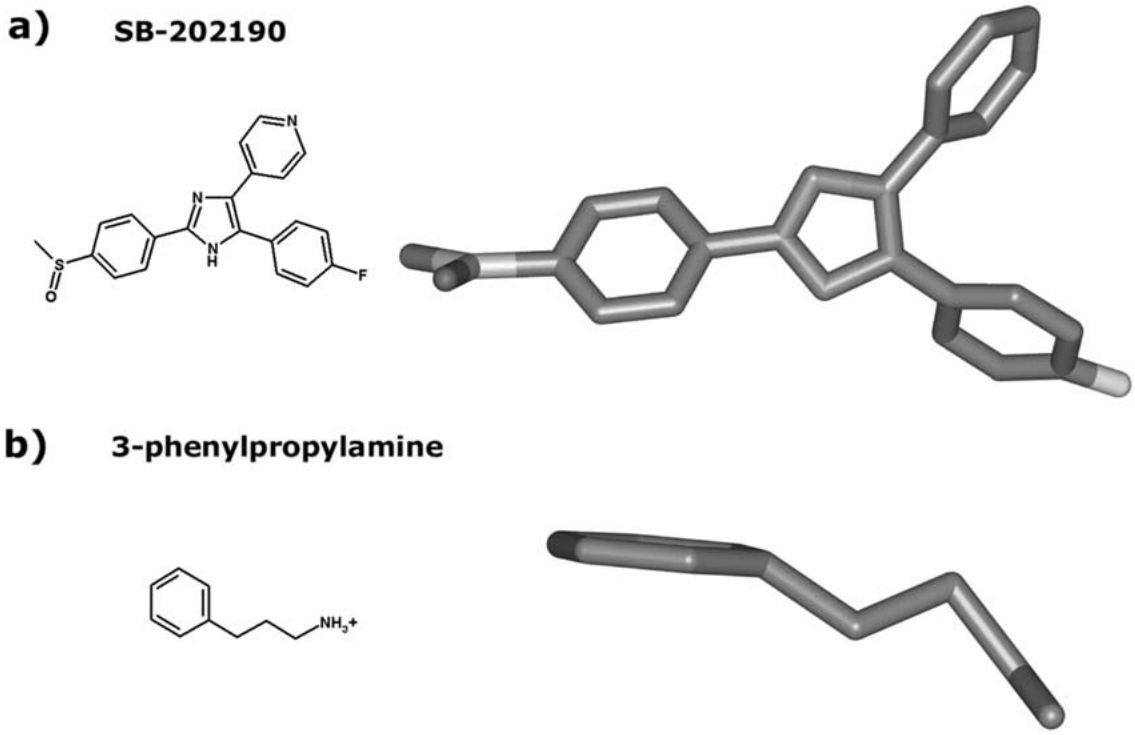

Figure 4. Two examples where the resolution of the complex is high (≤2.0 Å) while the structures are wide of the mark. (a) When analyzing SB-202190 it is clear that the structure is wrong. The methanesulfinyl moiety is planar instead of the preferred pyramidal. The temperature factors for this part of the ligand are higher (>33) than the cut-off allowed here. The conformational energy difference between the pyramidal and planar forms was calculated to be as high as 41.9 kcal/mol (HF/6-31G*), in favor of the 'pyramidal' form. This high conformational energy is clearly incompatible with the high affinity (30.8 nM) of SB-202190 binding to P38 Map kinase [23]. (b) It can be seen that the benzene carbon next to the propyl-amine moiety of 3-phenylpropylamine is pyramidal, instead of a planar. The temperature factors for this part of the ligand are high (>40). Hydrogens are removed for clarity.

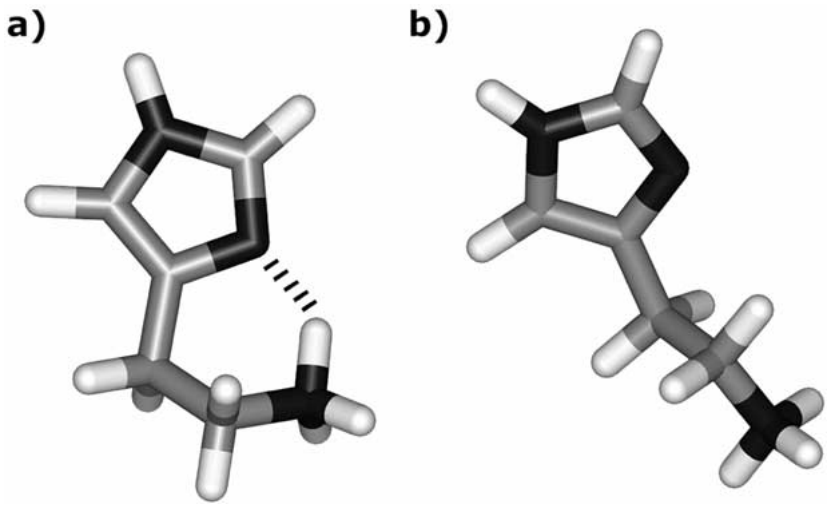

Figure 5. Compound **4** is not present in the MMFF94S gas phase ensemble but is in the MMFF94S\GB/SA ensemble. The global energy minima (a) of **4** in gas phase and in solution are almost identical. The energy difference between lowest energy conformation and the bioactive conformation (b) in gas phase is 13.4 kcal/mol, which is above the energy cut-off (12 kcal/mol). Though a folded conformation is still the global minimum, the extra competition between solute–solvent interactions and intramolecular hydrogen bonds, reduce the energy difference to only 1.5 kcal/mol when using GB/SA. This is well within the defined energy cut-off.

fied X-ray conformation were in all cases greater than 0.5 Å. Thus, these ligands do not bind in a local minimum conformation, according to AMBER*\GB/SA. Macromodel's default setting is to attempt to converge the structures. That is, each conformer obtained generally lies at or very close to a local minimum on the potential hypersurface. To illustrate, Figure 6 shows a cartoon where the potential energy (E) changes with some conformational parameter (R). If the energy well is broad, conformations which may be geometrically far from a local minimum (Figure 6a), but close energetically will be missed by a method like AMBER*\GB/SA, which tries to find only local minima (Figure 6b). This effect will tend to be more pronounced the larger the molecule becomes.

Catalyst

Both FAST and BEST produce mediocre results. FAST manages to reproduce sixteen of the bioactive conformations, whereas BEST reproduces fifteen (Tables 2 and 3). Again, none of the seven ligands with eight or more torsional angles were found. When comparing the two methods, it is intriguing to note that FAST actually gives one more hit than BEST. Bear in mind that FAST produces the results in six minutes, whereas the calculations performed with BEST took almost five hours (Tables 2 and 3). Perhaps BEST might work better than FAST when analyzing a different data set, for example one including more complex ring-systems, which is reported to be where its strength lies. Nonetheless, for systems like these, FAST outperforms BEST. It is worth noting that Catalyst's results appear to be completely independent of the input conformation.

As mentioned above, the poling algorithm distorts the potential energy hypersurface. It does so by putting a 'pole', an extra energy penalty function, wherever it has previously been on the potential hypersurface. Thus, geometrically similar conformations are prevented from being sampled. This non-physical function might be one explanation for its mediocre performance. When using BEST, one has the option to turn off the poling algorithm. When not using the poling function, two additional hits were obtained (**16**, **21**), suggesting that poling is not an advantage in this context.

Confort

The results for the Confort diverse conformational ensembles are poor. The ensembles generated in order to favor conformational diversity (by using the energy filter last) show poorer performance, than the single representative conformation retrieved by Corina (Tables 2 and 3). The results improved (11 hits), when priority was given to low-energy conformations (by using the intermediate energy filter). Note that the latter method is significantly slower than the first method (Tables 2 and 3). This is due to the fact that the energy has to be evaluated for each generated conformation.

To give a limit on how many hits can possibly be achieved, all of the generated conformers within an energy window of 15 kcal/mol were collected. By doing this, the average number of conformations was increased from 23 to 169. Four additional hits were obtained, resulting in a total of 15 hits. Thus, sampling of diverse conformations, by optimizing certain interatomic distances, does not seem to be expedient for reproducing bioactive conformations.

Flo99

The input conformation given to Flo99 was found to influence the generated ensembles slightly (Tables 2 and 3). When using the relaxed X-ray structures as the starting conformation, 21 hits were found. When using input structures generated with the 2D-to-3D generator, 20 hits were obtained. Thus, Flo99 performs almost as well as AMBER*\GB/SA, despite the crudeness of simply ignoring electrostatic effects. An additional bonus is that the average number of conformations retrieved by Flo99 is half that of AMBER*, in a tenth of the CPU time. Moreover, Flo99 is the only method which reproduces the bioactive conformation of a ligand having eight or more rotatable bonds (compound **27**, Table 2).

Omega

The input conformation given to Omega was found to strongly influence the generated ensembles. Using the relaxed X-ray structures as input, 17 hits were found. However, using input structures generated with the 2D-to-3D generator gave only 13 hits. The reason is that Omega does not modify the input bond lengths or angles. Omega deconstructs the molecule into fragments, and these fragments are subsequently put back together, according to certain rules, without optimizing bond lengths and angles. Obviously, bond lengths and angles are dependent to some extent on torsional angles. Thus, using the almost perfect input conformations from the optimized X-ray structures causes a bias. To check whether this was the case, a third

Table 2. The best fit, defined by lowest RMS deviation, compared with the unmodified X-ray structure, for ligands **1–32**, for all methods. The input conformation was derived from the X-ray structure.

Structure	Number of rotatable bonds	Catalyst		Confort		Flo99	MacroModel				OMEGA	Corina	Concord
		FAST	BEST	intermediate energy filter[a]	final energy filter[b]		MMFF94S		AMBER*		Beam		
							in vacuo	GB/SA	*in vacuo*	GB/SA			
No		**RMS**		**RMS**		**RMS**	**RMS**				**RMS**	**RMS**	**RMS**
1	1	0.16	0.35	0.21	0.64	0.23	0.10	0.10	0.10	0.09	0.11	0.42	0.34
2	1	0.07	0.10	0.11	0.51	0.08	0.09	0.09	0.10	0.08	0.08	0.12	0.12
3	1	0.15	0.14	0.22	0.10	0.22	0.23	0.22	0.23	0.23	0.22	0.22	0.22
4	2	0.15	0.16	0.13	0.68	0.12	0.66	0.20	0.34	0.25	0.26	0.12	0.12
5	3	0.14	0.14	0.92	0.16	0.36	1.21	0.23	1.07	0.37	0.41	1.18	0.95
6	3	0.66	0.55	1.57	1.72	0.26	0.41	0.41	0.20	0.33	0.15	1.48	1.67
7	3	0.12	0.11	0.83	1.01	0.31	0.12	0.13	0.15	0.16	0.20	0.91	0.95
8	3	0.43	0.36	0.32	0.32	0.24	0.22	0.29	0.27	0.31	0.44	0.57	0.51
9	4	0.44	0.30	0.39	0.85	0.29	0.30	0.32	0.36	0.28	0.44	0.39	0.53
10	4	0.43	0.29	0.37	0.85	0.32	0.33	0.35	0.33	0.27	0.41	0.38	0.49
11	4	0.49	0.39	0.40	0.48	0.35	0.34	0.34	0.27	0.25	0.67	0.91	0.69
12	4	0.48	0.19	0.50	0.57	0.40	1.02	0.12	0.84	0.46	0.72	0.63	1.34
13	4	1.29	0.75	0.99	0.49	0.50	0.35	0.33	0.44	0.61	0.34	0.34	0.47
14	4	0.97	0.44	0.72	2.00	0.49	0.41	0.39	0.36	0.98	0.53	1.64	1.72
15	4	0.47	0.52	1.18	1.10	0.71	0.70	0.85	1.53	1.55	0.75	1.17	1.44
16	5	0.45	0.57	0.69	0.47	0.78	0.72	0.69	0.36	0.31	0.31	0.50	0.58
17	5	0.50	0.83	0.91	0.85	0.35	0.55	0.73	0.40	0.42	0.46	1.01	1.10
18	5	0.82	0.67	0.39	0.58	0.23	0.28	0.12	0.30	0.26	0.33	1.00	0.87
19	5	0.31	0.35	0.39	0.39	0.37	0.93	0.44	0.43	0.48	0.63	0.60	0.97
20	5	0.79	0.77	1.11	2.53	0.71	0.59	0.61	0.53	0.49	0.87	2.16	1.76
21	5	0.67	0.67	1.04	1.43	0.40	0.47	0.22	0.76	0.23	0.47	2.07	0.89
22	5	0.46	0.35	0.87	2.19	0.27	0.96	0.21	0.36	0.20	0.65	2.11	0.55
23	5	0.82	0.47	1.00	1.04	0.35	0.50	0.56	0.30	0.27	0.69	0.40	0.83
24	6	0.89	0.80	0.38	0.78	0.42	0.27	0.26	0.33	0.35	0.46	1.00	0.91
25	7	0.46	0.59	0.50	0.86	0.57	0.77	0.68	1.46	0.48	0.49	0.58	0.54
26	8	1.01	1.26	0.81	2.57	0.81	1.17	0.57	1.44	0.89	1.99	1.91	1.61
27	8	0.86	1.09	1.23	2.13	0.25	2.39	0.97	2.36	1.06	1.29	2.89	2.63
28	8	0.98	0.84	1.57	2.08	0.71	1.73	1.23	1.96	1.20	1.52	2.75	3.01
29	8	0.81	0.96	2.16	1.70	0.90	1.09	0.70	1.01	0.84	0.63	2.09	2.79
30	10	0.94	1.20	1.99	1.37	1.12	1.02	0.85	0.96	0.75	2.01	2.59	2.78
31	11	1.17	1.31	1.34	2.62	1.09	0.69	0.71	1.18	0.96	1.12	2.47	2.40
32	11	1.48	1.44	1.45	0.92	0.53	2.37	0.79	1.74	0.60	0.87	2.71	3.55
Hits		**16**	**15**	**11**	**7**	**21**	**14**	**19**	**19**	**22**	**17**	**8**	**6**
CPU time (s)		332[c]	17171[c]	11814[d]	364[d]	3035[d]	24211[d]	35439[d]	23389[d]	36130[d]	21.2[d]	n.d.	n.d.
Ave. confs		55	84	23	6	70	80	144	96	154	30	1	1

[a]Using the '-e' option. [b]Using the '-E' option. [c]IRIX Release 6.5, MIPS R10000 Processor, 180 MHz. [d]IRIX Release 6.5, MIPS R10000 Processor, 250 MHz.

Table 3. The best fit, defined by lowest RMS deviation, compared with the unmodified X-ray structure, for ligands **1–32**, for all methods. The input conformation was generated with the 2D-to-3D-generator program Corina.

Structure	Number of rotatable bonds	Catalyst		Confort		Flo99	MacroModel				OMEGA	Corina	Concord
		FAST	BEST	intermediate energy filter[a]	final energy filter[b]		MMFF94S		AMBER*		Beam		
							in vacuo	GB/SA	*in vacuo*	GB/SA			
No		**RMS**		**RMS**		**RMS**	**RMS**				**RMS**	**RMS**	**RMS**
1	1	0.16	0.35	0.21	0.64	0.22	0.10	0.10	0.10	0.09	0.42	0.42	0.34
2	1	0.07	0.10	0.11	0.51	0.09	0.09	0.09	0.10	0.09	0.08	0.12	0.12
3	1	0.15	0.14	0.22	0.10	0.22	0.23	0.22	0.23	0.21	0.22	0.22	0.22
4	2	0.15	0.16	0.13	0.68	0.13	0.66	0.20	0.34	0.25	0.26	0.12	0.12
5	3	0.14	0.14	0.77	0.16	0.49	1.21	0.23	1.07	0.37	0.44	1.18	0.95
6	3	0.66	0.55	1.57	1.72	0.40	0.41	0.41	0.32	0.33	0.51	1.48	1.67
7	3	0.12	0.11	0.83	1.01	0.30	0.12	0.13	0.15	0.16	0.47	0.91	0.95
8	3	0.43	0.36	0.29	0.29	0.24	0.22	0.29	0.27	0.31	0.44	0.57	0.51
9	4	0.44	0.30	0.40	0.85	0.30	0.30	0.32	0.37	0.28	0.48	0.39	0.53
10	4	0.43	0.29	0.37	0.85	0.32	0.33	0.35	0.33	0.27	0.46	0.38	0.49
11	4	0.49	0.39	0.40	0.61	0.35	0.33	0.34	0.27	0.25	0.64	0.91	0.69
12	4	0.48	0.19	0.50	0.57	0.40	1.02	0.12	0.84	0.46	1.00	0.63	1.34
13	4	1.29	0.75	0.99	0.49	0.53	0.35	0.33	0.44	0.61	0.36	0.34	0.47
14	4	0.97	0.44	0.72	2.01	0.58	0.41	0.39	0.36	0.98	1.91	1.64	1.72
15	4	0.47	0.52	1.19	1.12	0.58	0.70	0.85	0.55	1.17	0.74	1.17	1.44
16	5	0.45	0.57	0.69	0.47	0.78	0.72	0.69	0.36	0.31	0.75	0.50	0.58
17	5	0.50	0.83	0.91	0.85	0.41	0.66	0.73	0.40	0.42	0.48	1.01	1.10
18	5	0.82	0.67	0.39	0.60	0.27	0.28	0.12	0.26	0.24	0.65	1.00	0.87
19	5	0.31	0.35	0.39	0.39	0.37	0.92	0.44	0.43	0.48	0.62	0.60	0.97
20	5	0.79	0.77	1.11	2.53	0.72	0.59	0.62	0.45	0.44	0.97	2.16	1.76
21	5	0.67	0.67	1.04	1.43	0.41	0.47	0.21	0.76	0.28	0.46	2.07	0.89
22	5	0.46	0.35	0.87	2.19	0.34	0.96	0.21	0.36	0.19	0.66	2.11	0.55
23	5	0.82	0.47	1.04	1.03	0.41	0.51	0.56	0.30	0.28	0.69	0.40	0.83
24	6	0.89	0.80	0.39	0.78	0.38	0.27	0.26	0.33	0.35	0.74	1.00	0.91
25	7	0.46	0.59	0.50	0.86	0.45	0.89	0.68	1.68	0.48	0.34	0.58	0.54
26	8	1.01	1.26	0.80	2.08	0.74	1.02	0.77	1.48	0.88	2.30	1.91	1.61
27	8	0.86	1.09	1.27	1.83	0.84	2.35	0.97	2.37	1.06	1.36	2.89	2.63
28	8	0.98	0.84	2.17	1.35	0.89	1.80	1.23	1.96	1.19	1.69	2.75	3.01
29	8	0.81	0.96	2.38	2.21	1.41	1.11	0.73	1.02	0.76	0.88	2.09	2.79
30	10	0.94	1.20	2.22	1.81	0.78	1.80	0.96	0.96	0.88	2.01	2.59	2.78
31	11	1.17	1.31	1.34	2.62	1.06	0.77	0.81	1.08	1.24	1.46	2.47	2.40
32	11	1.48	1.44	1.38	2.31	1.24	2.24	0.84	2.28	0.68	0.96	2.71	3.55
Hits		**16**	**15**	**11**	**6**	**20**	**14**	**19**	**20**	**22**	**13**	**8**	**6**
CPU time (s)		332[c]	17157[c]	11136[d]	364[d]	3041[d]	24549[d]	36900[d]	23910[d]	37663[d]	18[d]	n.d.	n.d.
Ave. confs		55	84	23	6	70	82	140	92	155	25	1	1

[a]Using the '-e' option. [b]Using the '-E' option. [c]IRIX Release 6.5, MIPS R10000 Processor, 180 MHz. [d]IRIX Release 6.5, MIPS R10000 Processor, 250 MHz.

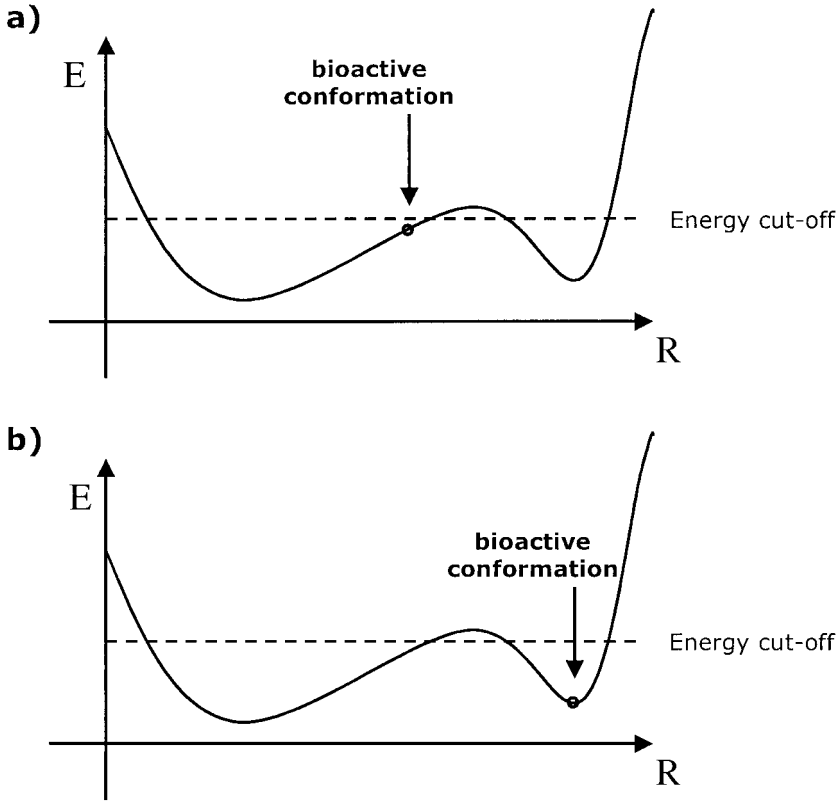

Figure 6. A cartoon of a conformational energy surface showing how the potential energy (E) changes with some conformational parameter (R). Two energy wells are shown, one broad and one narrow. Bioactive conformations which are geometrically far from a local minimum (a) will be missed by a method which tries to find only local minima. That is, even though the bioactive conformation is well within the energy threshold it will be missed (a), while the bioactive conformation in (b) will be sampled. Compounds **13–15** and **26–32** do not bind in a local minimum conformation, according to AMBER*\GB/SA.

input to Omega was manufactured, using structure **16** as a test. Here, the input conformation was that produced by Corina, i.e., 2D-to-3D conversion. But then, the bond angles were altered by hand to those found in the optimized X-ray structure. A new search was conducted. This time the bioactive conformation was found (0.27 Å RMSD). Reason being, that a greater number of conformations were generated, and that the Corina bond angles exclude certain conformations on the basis of van der Waals clashes.

One could claim that the Omega approach is a little too simplistic. However, keep in mind that Omega is designed specifically to have a high information/CPU ratio. The conformational searches for all 32 compounds totaled less than 22 sec. By contrast, some of the more sophisticated methods ran for hours of CPU time, and delivered only a small margin of statistical improvement in reproducing bioactive conformations.

Representing the ensemble by a single conformation

Two frequently used rule-based methods, Concord [28] and Corina, normally produce just a single conformation. Conformational 'ensembles' represented by a single conformation are included in Tables 2 and 3 for the purposes of comparison. Significantly, neither developing group claims that their goal, with their 2D-to-3D converter, is to reproduce bioactive conformations. Rather, their aim is to generate one reasonable low-energy conformation. Nonetheless, it is interesting to see how well these single conformations compare to multiconformational ensembles.

Concord and Corina reproduce around a fifth of the bioactive conformations used in this study (Tables 2 and 3). Corina is performing slightly better than Concord. The compounds that are reproduced are, as expected, those which include few torsional degrees of freedom. As an aside, it might arguably be better to use rule-based conformer generation, rather

Table 4. The number of structures in 0.25 Å intervals when starting from the relaxed X-ray structure.

	Catalyst		Confort		Flo99	MacroModel				OMEGA
	FAST	BEST	intermediate energy filter[a]	final energy filter[b]		MMFF94S		AMBER*		Beam
						in vacuo	GB/SA	*in vacuo*	GB/SA	
RMS	**Hits**		**Hits**		**Hits**	**Hits**				**Hits**
<0.25	6	6	4	2	6	5	10	5	6	5
0.25-0.50	10	9	7	5	15	9	9	14	16	12
0.50-0.75	3	6	4	5	6	7	8	1	2	7
0.75-1.00	9	6	6	6	3	3	4	3	5	3
1.00-1.25	2	2	5	3	2	5	1	3	2	1
1.25-1.50	2	3	2	2	0	0	0	2	0	1
1.50-1.75	0	0	2	2	0	1	0	2	1	1
1.75-2.00	0	0	1	0	0	0	0	1	0	1
>2.00	0	0	1	7	0	2	0	1	0	1
Hits	**16**	**15**	**11**	**7**	**21**	**14**	**19**	**19**	**22**	**17**

[a]Using the '-e' option. [b]Using the '-E' option.

than global minimum conformations, when calculating 3D descriptors [29], since the former generates conformers in a consistent manner. In keeping with this, the global minimum conformations obtained from AMBER*\GB/SA gave eight hits, and the RMSDs were generally higher (results not shown). Thus, Corina performs as well as or better than simply using global minimum conformations according AMBER*\GB/SA.

Fine tuning of conformational ensembles

This study solely investigates how well the different methods perform when using default settings. An obvious subsequent study is to attempt to optimize the conformational ensemble sizes. That is, to investigate whether modifying the parameters which control the ensemble size may lead to smaller ensembles with a higher probability of finding the bioactive conformation in the generated ensemble. Such detailed studies are in progress and will be reported elsewhere.

The present data set comprise diverse proteins and ligands it may thus be appropriate to draw general conclusions. Accordingly, the results obtained here point out in which direction one should proceed to ensure valid conformational searching. Three particular observations highlight that geometrically similar structures should be collected, with less regard to convergence: (i) even the best method in terms of retrieval (AMBER*\GB/SA) failed to find almost a third of the bioactive conformations because these structures were not present in the crystal as local minima; (ii) the methods supporting diverse sampling (Catalyst and Confort) performed least well; (iii) more hits were retrieved when giving priority to low-energy conformations as opposed to conformational diversity (Confort). We have previously reported on a study where we analyzed a number of experimentally determined ligand–protein complexes [25]. The internal energy required for the ligand to adopt the bioactive conformation was in most cases found to be below 3 kcal/mol. The inference is that a larger conformational penalty is an impediment to high-affinity binding. Thus, the use of stricter energy cut-offs is important, to reduce the number of energetically inaccessible conformations, so long as the force field is a good description of the true energy surface. In addition, we suggest that collecting a range of structures within flat energy wells increases the probability of having the bioactive conformation in the generated ensembles.

It is discouraging that the fairly approximate method implemented in Flo99, which completely ignores coulombic and solvation effects, performs almost as well as the more sophisticated method AMBER*\GB/SA which includes these effects. The molecular electrostatics are an important determinant of the solvation energies of conformational isomers. The molecular description in the GB/SA model assigns partial atomic charges to account for electrostatics. The shortcoming here is that the partial charges are assigned according to atom type, and are therefore independent of the conformation. Besides, these charges are static, and cannot relax in response to the local environment (polarization). It is likely that polarization effects need to be included in the force field definitions, in order to improve the quality of the calculations [30].

Table 5. The number of structures in 0.25 Å intervals when starting from the 2D-3D structure.

	Catalyst		Confort		Flo99	MacroModel				OMEGA
	FAST	BEST	intermediate energy filter[a]	final energy filter[b]		MMFF94S		AMBER*		Beam
						in vacuo	GB/SA	*in vacuo*	GB/SA	
RMS	**Hits**		**Hits**		**Hits**	**Hits**				**Hits**
<0.25	6	6	4	2	5	5	10	4	6	2
0.25-0.50	10	9	7	4	15	9	9	16	16	11
0.50-0.75	3	6	4	6	5	6	6	1	2	8
0.75-1.00	9	6	6	5	4	4	6	3	4	4
1.00-1.25	2	2	4	3	2	4	1	3	4	1
1.25-1.50	2	3	3	2	1	0	0	1	0	2
1.50-1.75	0	0	1	1	0	0	0	1	0	1
1.75-2.00	0	0	0	2	0	2	0	1	0	1
>2.00	0	0	3	7	0	2	0	2	0	2
Hits	**16**	**15**	**11**	**6**	**20**	**14**	**19**	**20**	**22**	**13**

[a]Using the '-e' option. [b]Using the '-E' option.

It is at times advocated that sampling as diverse a conformation space as possible is more appropriate for certain applications. For example, for applications such as 3D-database searching and rigid-fit pharmacophore modeling, a much more diverse set of conformations is recommended. However, the results here cast doubt on the reliability of diverse ensembles when generating conformations with a view of performing 3D database searches or building a pharmacophore model – a more challenging problem than retrieving bioactive conformations. Additional features, like Catalyst's poling algorithm and Confort's refinement procedure, do not seem to increase the likelihood of retrieving the bioactive conformation; on the contrary, this study indicates that they have a negative impact. Thus, it seems one can obtain adequate diversity in terms of molecular shape, simply by sampling low-energy conformations.

Conclusions

Several programs (Catalyst, Confort, Flo99, MacroModel, and Omega) have been evaluated for their ability to reproduce bioactive conformations of protein-bound ligands. The ligands from 32 diverse high-quality X-ray complexes have been analyzed.

The Low-Mode Conformational Search method (with AMBER* and the GB/SA hydration model), as implemented in MacroModel, was found to perform better than other algorithms. Moreover, by including a solvation model, the hit rates increases (MMFF94S and AMBER*). This is due to reducing the significance of intramolecular electrostatic interactions. Completely ignoring them has a similarly beneficial effect for less cost (Flo99). Confort and Catalyst, with diverse conformational sampling, performed least well. Giving priority to low-energy conformations as opposed to diverse conformations was found to result in more hits (Confort). Remarkably, Catalyst's FAST algorithm slightly outperformed the BEST algorithm. The rule-based method Omega, which is several orders of magnitude faster than the more sophisticated methods, also achieved reasonable accuracy. However, Omega was found to be dependent on the input conformation. It proved difficult to retrieve structures having eight or more rotatable bonds for all methods. According to AMBER*\GB/SA these protein-bound ligands do not bind in energy minimum conformations. Finally, the results obtained here indicate that geometrically similar structures should be collected in order to increase the probability of finding the bioactive conformation among the generated ensembles.

Acknowledgements

The helpful advice from Drs Jeremy Greenwood, Volker Schnecke, Jens Sadowski, Andrew Grant, and Morten Langgård is gratefully acknowledged.

References

1. a. Martin, Y.C., J. Med. Chem., 35 (1992) 2145. b. Martin, Y.C., Bures, M.G. and Willett, P., In Lipkowitz, K.B., Boyd, D.B. (eds), Reviews in Computational Chemistry, VCH Publishers, New York, 1990, pp. 213–263.

2. Marshall, G.R., Barry, C.D., Bosshard, H.E., Dammkoehler, R.A. and Dunn, D.A., in Olsen E.C., Christoffersen R.E. (eds), Computer-Assisted Drug Design., American Chemical Society Symposium: Washington DC, 1979, pp. 205–226.
3. a. Kuntz, I.D., Blaney, J.M., Oatley, S.J., Langridge, R. and Ferrin, T.E., J. Mol. Biol., 265 (1982) 269. b. Stoichet, B.K., Stroud, R.M., Santi, D.V., Kuntz, I.D. and Perry, K.M., Science, 259 (1993) 1445.
4. a. Vedani, A., McMasters, D.R. and Dobler, M., Quant. Struct.-Act. Relat., 19 (2000) 149. b. Guccione, S., Doweyko, A.M., Chen, H., Barretta, G.U. and Balzano, F., J. Comput. Aid. Mol. Des., 14 (2000) 647.
5. Allen, F.H., Davies, J.E., Galloy, J.J., Johnson, O., Kennard, O., Macrae, C.F., Mitchell, E.M., Mitchell, G.F., Smith, J.M., and Watson, D.G., J. Chem. Inf. Comput. Sci., 31 (1991) 187.
6. Corina, Molecular Networks, GmbH Computerchemie Langemarckplatz 1, Erlangen, Germany.
7. Sadowski, J., Gasteiger, J. and Klebe, G., J. Chem. Inf. Comput. Sci., 34 (1994) 1000.
8. MacroModel V7.0: Mohamadi, F., Richards, N.G.J., Guida, W.C., Liskamp, R., Lipton, M., Caufield, C., Chang, G., Hendrikson, T. and Still, W.C., J. Comput. Chem., 11 (1990) 440.
9. SYBYL molecular modeling software; TRIPOS Inc., 1699 South Hanley Road, Suite 303, St. Louis MO 63144.
10. Treasurywala, A.M., Jaeger, E.P. and Peterson, M.L., J. Comput. Chem., 17 (1996) 1171.
11. Leach, A., in Lipkowitz, K.B., Boyd, D.B. (eds), Reviews in Computational Chemistry, VCH Publishers, New York, 1991, pp. 1–47.
12. Bernstein, F., Koetzle, T.F., Williams, G.J.B., Meyer Jr, E.F., Brice, M.D., Rodgers, J.R., Kennard, O., Schimanouchi, T. and Tasumi, M.J., J. Mol. Biol., 112 (1977) 535.
13. Hendlich, M., Acta Crystallographica D54 (1998) 1178. Relibase is copyright Manfred Hendlich 1994–1999 and Cambridge Crystallographic Data Centre 1999, 2000.
14. The Omega program is available from OpenEye Science Software, 335c Winische Way, Santa Fe, NM 87501, U.S.A.
15. a. Spraque, P.W., Perspect. Drug Disc. Des. 3 (1995) 1. b. Spraque, P.W. and Hoffman, R., in Waterbeemd, H., Testa, B. and Folkers, G. (eds), Computer-Assisted Lead Finding and Optimization, VHCA, Basel, 1990, pp. 223–230.
16. Pearlman, R.S. and Balducci, R., Confort User's Manual, distributed by Tripos Inc., St. Louis, MO, U.S.A.
17. a. McMartin, C. and Bohacek, R. J. Comput. Aid. Mol. Des., 11 (1997) 333. b. McMartin, C. and Bohacek, R., J. Comput. Aid. Mol. Des., 9 (1995) 237.
18. Smellie, A., Teig, S.L., and Towbin, P., J. Comp. Chem., 16 (1995) 171.
19. Metropolis, N., Rosenbluth, A.W., Rosenbluth, M.N., Teller, A.H. and Teller, E., J. Chem. Phys., 21 (1953) 1087.
20. a. Kolossváry, I. and Guida, W.C., J. Am. Chem. Soc., 118 (1996) 5011. b. Kolossváry I. and Guida, W.C., J. Comput. Chem., 20 (1999) 1671.
21. Still, W.C., Tempczyk, A., Hawley, R.C. and Hendrickson, T., J. Am. Chem. Soc., 112 (1990) 6127.
22. Personal communication, Jens Sadowski, AstraZeneca R&D Mölndal, Sweden.
23. SPARTAN 5.1, Wavefunction, Inc.18401 Von Karman Ave., Ste. 370, Irvine, CA 92612 U.S.A.
24. Fox, T., Coll, J.T., Xie, X., Ford, P.J., Germann, U.A., Porter, M.D., Pazhanisamy, S., Fleming, M.A., Galullo, V., Su, M.S. and Wilson, K.P., Protein Sci., 7 (1998) 2249.
25. Boström, J., Norrby, P.-O. and Liljefors, T., J. Comput.-Aided. Mol. Des., 12 (1998) 383.
26. Kurinov, I.V. and Harrison, R.W., Nat. Struct. Biol., 1 (1994) 735.
27. Xu, Z., Bernlohr, D.A. and Banaszak, L.J., J. Biol. Chem., 268 (1993) 7874.
28. Pearlman, R.S., Concord User's Manual, distributed by Tripos Inc., St. Louis, MO, U.S.A.
29. Pastor, M., Cruciani., G., McLay, I., Pickett, S. and Clementi, S., J. Med. Chem., 43 (2000) 3233.
30. a. Howard, A.E., Singh, U.E., Billeter, M. and Kollman, P.A., J., Am. Chem. Soc., 110 (1988) 6984. b. Meng, E.C., Cieplak, P., Caldwell, J.W. and Kollman, P.A., J. Am. Chem. Soc., 116 (1994) 12061.